Organic & Biomolecular Chemistry

RSC Publishing

PAPER

View Article Online
View Journal | View Issue

The first ratiometric fluorescent probes for aminopeptidase N cell imaging†‡

Cite this: *Org. Biomol. Chem.*, 2013, **11**, 378

Laizhong Chen, Wei Sun, Jing Li, Zhenzhen Liu, Zhao Ma, Wei Zhang, Lupei Du, Wenfang Xu, Hao Fang and Minyong Li*

Received 7th August 2012,
Accepted 5th November 2012

DOI: 10.1039/c2ob26564h

www.rsc.org/obc

In the current paper, three activity-based colorimetric and ratiometric fluorescent probes based on a naphthalimide fluorophore were well designed and synthesized, which can be recognized and hydrolyzed by aminopeptidase N (APN) at both the enzymatic and cellular level by following the fluorescent emission wavelength change from blue to green light. As a result, these molecules were successfully identified as the first ratiometric fluorescent probes for APN cell imaging.

Introduction

Aminopeptidase N (APN, EC 3.4.11.2), which belongs to the M1 family of the MA clan of peptidases, is a Zn^{2+} dependent exopeptidase that degrades preferentially proteins and peptides with an N-terminal neutral amino acid.[1,2] It should be underlined that APN, which is highly expressed in tumor cells, has been demonstrated to perform a vital role in tumor invasion, metastasis and angiogenesis,[3–7] and has become a diagnostic or prognostic biomarker for cancers.[8] Moreover, APN had been demonstrated to hold a critical position as a biomarker for cancer stem cells.[9]

Hitherto, many efforts have been undertaken to understand the distribution of APN and enhancing the imaging of APN in cancer tissues,[8,10–18] of which, the fluorescence-based imaging approach has exclusive advantages since it presents a real-time examination, displays a reasonable sensitivity, and provides a high spatiotemporal resolution. However, the reported fluorescent imaging probes for APN are all NGR (Asn-Gly-Arg) based affinity probes,[11–13,15,18] which can image APN in cancer cells or in mice with a high background signal, in such a way that it will significantly interfere with the imaging quality. By contrast, activity-based fluorogenic probes, which are non-fluorescent themselves and become fluorescent when degraded by their targeting peptidases, can reduce the non-specific background signal.[19] Moreover, probes with a dual emission are particularly viable because they enable a built-in calibration for environmental effects.[20,21] We have reported the first ratiometric fluorescent probe, **Ala-PABA-7HC**, which could detect the activity of aminopeptidase N (APN) at both the enzymatic and the cellular level with minimal environmental influence.[22] Nevertheless, **Ala-PABA-7HC** was not suitable to be implemented in cell imaging considering that the maximum emission peaks of both **Ala-PABA-7HC** (390 nm) and the releasing fluorophore **7HC** (450 nm) are in the wavelength range of blue light. Herein, we would like to describe a novel series of ratiometric fluorescent probes based on an intramolecular charge transfer (ICT) mechanism, which can be used to image APN in cancer cells.

Result and discussion

To find an activity-based fluorescent probe for APN, we chose 1,8-naphthalimide, a prototype intramolecular charge transfer (ICT) fluorophore as a reporter due to its advantageous optical properties, such as strong absorption and emission in the visible region, high photostability, large Stokes shift and insensitivity to pH.[23,24] Alanine and norvaline, which are favored by APN's activity site,[25] were chosen as the recognition moieties. The electron-withdrawing amide group weakened the ICT effect and resulted in a fluorescent emission wavelength blue shift. After the cleavage of the amide bond between the amino acids and the fluorophores by APN, 1,8-naphthalimide can be released in a non-reversible manner to emit a strong bright green fluorescence (Scheme 1). In this research, all of the three probes were efficiently synthesized (Scheme 2) and well characterized as depicted in the experimental and supplementary parts.

After carefully examining the spectroscopic properties in Tris-HCl buffer (100 mM, pH 7.5), the absorption spectra of these three probes and their fluorophores were found to have

Department of Medicinal Chemistry, Key Laboratory of Chemical Biology of Natural Products (MOE), School of Pharmacy, Shandong University, Jinan, Shandong 250012, China. E-mail: mli@sdu.edu.cn; Tel: +86-531-8838-2076

†This article is dedicated to Professor Wenfang Xu on the occasion of his 60th birthday.

‡Electronic supplementary information (ESI) available: Experimental procedures, ^{1}H NMR, ^{13}C NMR and HR-MS spectra. See DOI: 10.1039/c2ob26564h

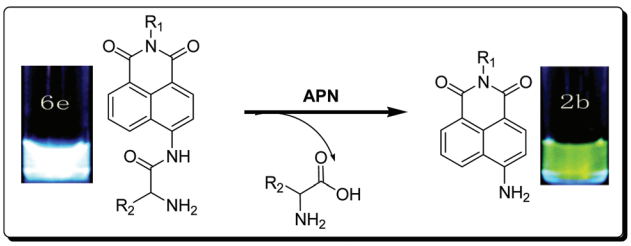

Scheme 1 Plausible detection mechanism of probes.

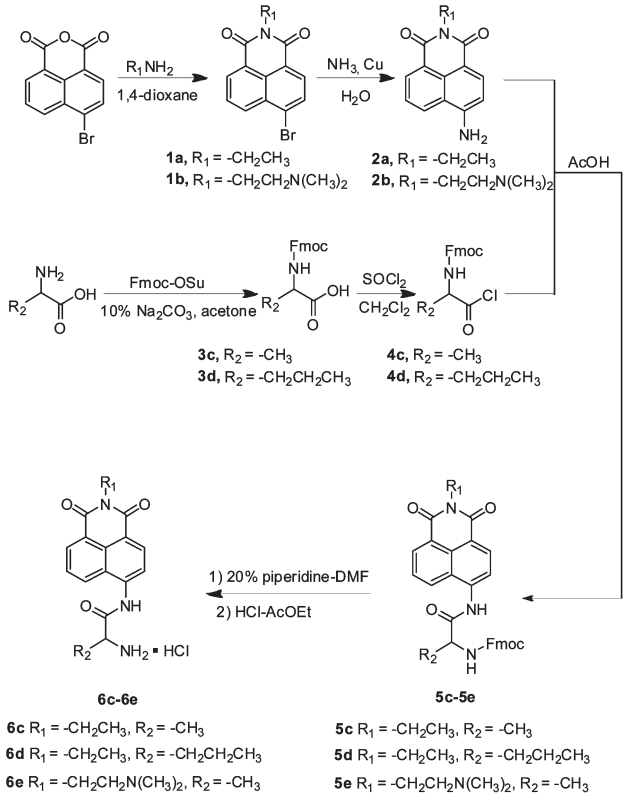

Scheme 2 Synthesis and structures of probes **6c**, **6d** and **6e**.

an intersection at a wavelength of 400 nm (Fig. 1). This interesting result envisions that they could be equally excited at this wavelength. When excited at 400 nm, the maximum emission wavelength of **6c**, **6d** and **6e** was at 460 nm, and that of **2a** and **2b** was at 550 nm (Fig. 2). The 90 nm shift indicated that these three molecules could be considered as candidates for ratiometric fluorescent probes.

In the enzymatic experiments, upon addition of porcine APN (0.2 IU) to the solution of **6e** (200 μM in 100 mM Tris-HCl, pH 7.5), the maximum emission peak experienced a red shift from 460 nm to 550 nm, and the ratio of fluorescence intensities (I_{550}/I_{460}) (λ_{ex} = 400 nm) meaningfully augmented from 0.45 to 4.67 (R = 10.4 fold) after 50 min (Fig. 3). Similar results were obtained as well when adding APN to the solution **6c** and **6d** (Fig. S1‡). Kinetics assays showed that all of the K_m values of the three probes (752.7 μM, 487.7 μM and 107.5 μM for **6c**, **6d** and **6e**, respectively) were lower than that of the commercial

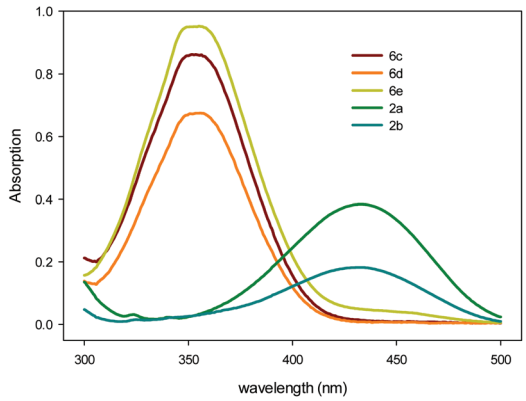

Fig. 1 Absorption spectra of **6c**, **6d**, **6e**, **2a** and **2b** (50 μM).

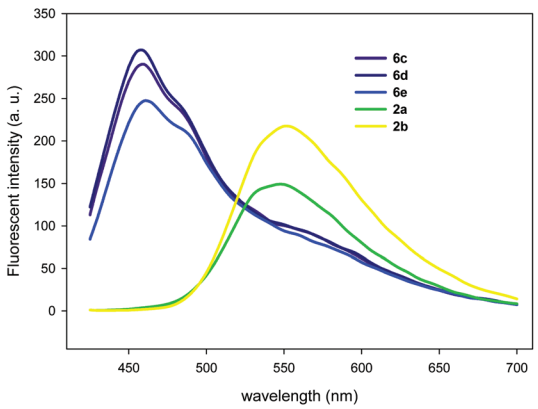

Fig. 2 Emission spectra of the probes **6c**, **6d**, **6e**, **2a** and **2b** (250 μM, excitation at 400 nm).

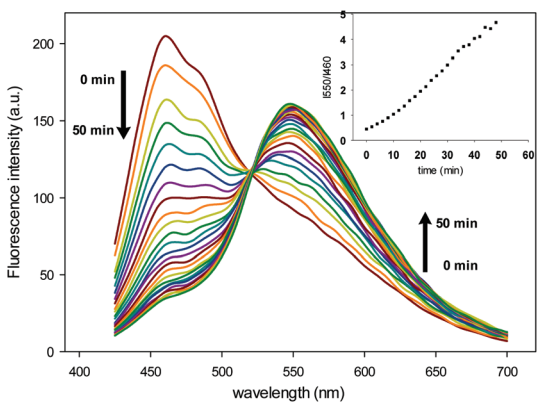

Fig. 3 Emission spectra of **6e** (200 μM) in the presence of APN (0.2 IU) in a Tris-HCl buffer (100 mM, pH 7.5). Inset: ratios of fluorescent intensities at 550 and 460 nm as a function of time after adding APN (λ_{ex} = 400 nm).

substrate L-Leu-*p*-nitroanilide (1180 μM), which indicates that the three probes may bind more strongly to APN than L-Leu-*p*-nitroanilide.[25] Because APN is also used as a biomarker to detect damage to the kidneys and is mainly located in the small-intestinal and renal microvillar membranes, the fluorescence probes should be stable enough to pass the gastrointestinal environment, then to arrive on the small intestinal

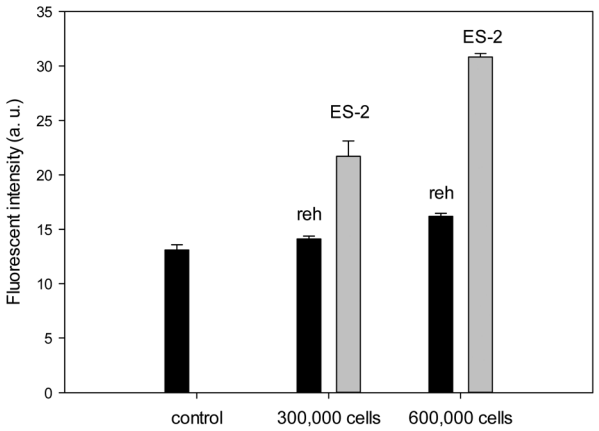

Fig. 4 Emission spectra of **6e** with ES-2 and REH cells. Cells and **6e** were suspended in RPMI-1640 medium and incubated at 37 °C for 1 h (λ_{ex} = 445 nm, λ_{em} = 550 nm).

membrane to express their activities. The stability test results (Fig. S3‡) disclosed that all of **6c**, **6d** and **6e** were stable in Tris-HCl buffer and artificial gastric juice. Moreover, there was no significant hydrolysis evidence of **6c** and **6e** in the artificial intestinal juice up to 5 h. All the above results confirmed that **6c**, **6d** and **6e** were successful ratiometric fluorescent probes for detecting the activity of APN in a neutral or acidic environment, and that **6c** as well as **6e** can also be used in artificial intestinal juice.

To further confirm the practical feasibility of our ratiometric fluorescent probes, we applied **6e** to the detection of APN activity in living cancer cells in view of its superior solubility, stability and lower K_m value. As demonstrated in Fig. 4, the fluorescence intensities of the solution of **6e** and APN high expressed ES-2 cells increased significantly after incubating for 1 h at 37 °C. However, compared to ES-2 cells, APN low expressed REH cells could hardly hydrolyze **6e** in the same conditions. This evidence indicated that **6e** could be applied in detecting APN activity in living cells, and may be used in ratiometric fluorescence imaging of endogenous APN. ES-2 cells incubated with the probe **6e** (5 μM) for 15 min disclosed an intensely blue fluorescence in the nucleus (Fig. 5B). The result revealed that the probe **6e** could penetrate the cell membrane and mainly label the nucleus. Moreover, a green intense fluorescence generated in the whole cells (Fig. 5C) illustrated that **6e** could be hydrolyzed by endogenous APN. In comparison, ES-2 cells incubated with both **6e** (5 μM) and the APN inhibitor, Bestatin (4.9 mM), for 15 min unveiled similar blue fluorescence in the nucleus but weak green fluorescence in the whole cells (Fig. 5G). The significant differences in ratio fluorescence responses in Fig. 5D and 5H clearly demonstrated that probe **6e** can be employed for ratiometric fluorescent imaging of endogenous APN in living cells (Fig. 5I).

Conclusions

In summary, three amino acid-naphthalimide probes were well designed and synthesized, and all of them could be recognized

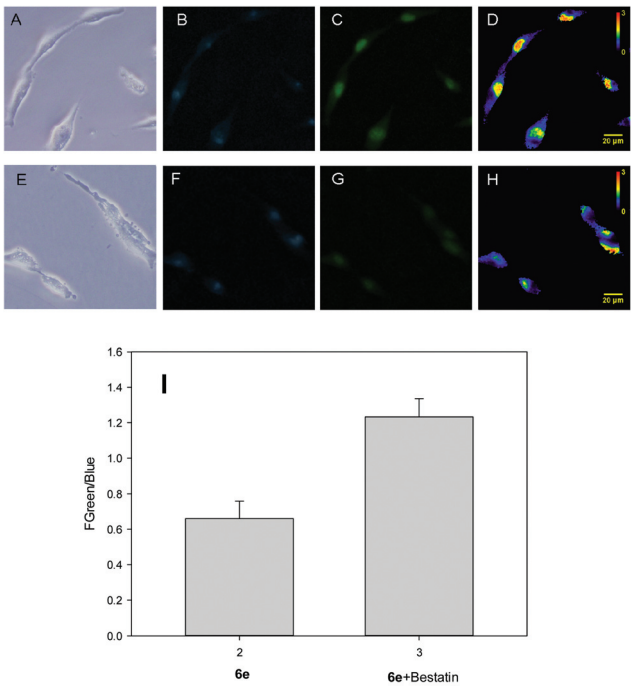

Fig. 5 Fluorescence images of living ES-2 cells: top row, ES-2 cells incubated with the probe **6e** (5 μM) for 15 min: (A) bright-field, (B) blue channel, (C) green channel, (D) ratio of (C) and (B); bottom row, ES-2 cells incubated with the probe **6e** (5 μM) and Bestatin (4.9 mM) for 5 min: (E) bright-field, (F) blue channel, (G) green channel, (H) ratio of (G) and (F). (I) Bars represent the mean ratio generated from the total integrated density from green channel over the total integrated density from blue channel. Error bars represent standard error measurement (s.e.m.).

and hydrolyzed by APN. These probes display a 90 nm red-shift of fluorescence emission and the color changes from colorless to olivinic upon addition of APN, and therefore can serve as colorimetric and ratiometric fluorescent probes for APN detection. One of them, **6e**, was also successfully applied in ratiometric fluorescent imaging of endogenous APN in living ES-2 cells. In view of the built-in correction ability for environmental interference, **6e** could be implemented as a useful diagnostic probe for APN high expressed cancer lines.

Experimental

1. Materials and instruments

All reagents were purchased from Acros and Aldrich. Twice-distilled water was used throughout all experiments. ^{1}H NMR and ^{13}C NMR were recorded on Bruker 300 NMR, 400 NMR and 600 NMR spectrometers. Mass spectra were performed by the analytical and the mass spectrometry facilities at Shandong University. Specific rotation was tested using a Anton Paar MCP200.

2. Synthesis of 6e

6-Bromo-2-(2-(dimethylamino)ethyl)-1*H*-benzo[*de*]isoquinoline-1,3(2*H*)-dione (1b). The solution of 4-bromo-1,8-naphthalic

anhydride (13.8 g, 50 mmol) and N^1,N^1-dimethylethane-1,2-diamine (5.28 g, 60 mmol) in 500 mL 1,4-dioxane was refluxed at 120 °C for 4 h. Then the mixture was cooled and poured into 500 mL water. The yielded yellowish sediments were collected by filtration and dried under 110 °C air atmosphere to obtain a pale-brown solid, 14.3 g, yield = 82.3%, mp: 142.5–143.5 °C.

6-Amino-2-(2-(dimethylamino)ethyl)-1*H*-benzo[*de*]isoquinoline-1,3-(2*H*)-dione (2b). The mixture of **1b** (1.7 g, 5 mmol), conc. ammonia (10 mL), copper power (0.032 g, 0.5 mmol) and a stirring bar were sealed in a 30 mL screwed tube and stirred in a oil bath at 100 °C for 10 h. After cooling to r.t., the suspension was extracted with 50 mL AcOEt, to the residue was added 50 mL water and extracted by another 50 mL AcOEt. The combination was washed with brine (100 mL × 1) and dried over anhydrous $MgSO_4$ for 24 h. The solution was concentrated under reduced pressure and then purified by combiflash to yield yellow power. Yield = 31.2%, mp: 222.9–225.1 °C.

2-((((9*H*-Fluoren-9-yl)methoxy)carbonyl)amino)propanoic acid (3c). To the solution of Ala (3.5 g, 40 mmol) in 120 mL 10% Na_2CO_3 was added the solution of FmocOSu (13.5 g, 40 mmol) in acetone (100 mL) at 0 °C. The mixture was stirred at r.t. overnight. Acetone was evaporated under reduced pressure and the residue was washed by ether (100 mL × 3). The water phase was adjusted to pH 2 with conc. HCl and extracted with AcOEt (100 mL × 3). The organic phase was dried over anhydrous $MgSO_4$ for 24 h. The solution was concentrated under reduced pressure and then recrystallized with AcOEt–*n*-hexane to yield a white solid, 10 g, yield = 80.4%, mp: 138.2–139.7 °C.

(9*H*-Fluoren-9-yl)methyl(1-chloro-1-oxopropan-2-yl)carbamate (4c). To the solution of **3c** (0.5 g, 1.6 mmol) in CH_2Cl_2 (8 mL) was added $SOCl_2$ (4 mL), the mixture was stirred at r.t. for 2 h. The solution was concentrated under reduced pressure and recrystallized with CH_2Cl_2–*n*-hexane to yield a white solid, 0.35 g, yield = 66.5%, mp: 94.5–96 °C.

(9*H*-Fluoren-9-yl)methyl(1-((2-(2-(dimethylamino)ethyl)-1,3-dioxo-2,3-dihydro-1*H*-benzo[*de*]isoquinolin-6-yl)amino)-1-oxopropan-2-yl)-carbamate hydrochloride (5e). The suspension of **4c** (0.96 g, 3.0 mmol) and **2b** (0.28 g, 1.0 mmol) in AcOH (20 mL) was refluxed for 4 h. The mixture was cooled and concentrated to 5 mL, 40 mL AcOEt was added to the solution. The yield precipitation was filtered and washed with 20 mL AcOEt to gain a deep yellow power. The deep yellow power was recrystallized with MeOH to yield a khaki powder, 0.15 g, yield = 26.0%, mp: 156.7–158.1 °C.

2-Amino-*N*-(2-(2-(dimethylamino)ethyl)-1,3-dioxo-2,3-dihydro-1*H*-benzo[*de*]isoquinolin-6-yl)propanamide dihydrochloride (6e). The mixture of **5e** (0.10 g, 0.16 mmol) and 5 mL 20% piperidine–DMF was stirred at r.t. for 30 min then concentrated under reduced pressure at 90 °C to remove excess piperidine and DMF. 5 mL EtOAc solution saturated with HCl gas was added and stirred at r.t. for 1 h. The yield precipitation was filtered and recrystallized with AcOEt–MeOH to yield a light yellow power, 30 mg, yield = 43.9%, mp: 255.3–257.8 °C, $[\alpha]_D^{20}$ = 16.09 (c = 0.087, MeOH). ^{1}H-NMR (DMSO, 300 MHz): δ 11.21 (s, 1 H), 9.60 (s, 1 H), 8.82 (d, 1 H, J = 8.1 Hz), 8.58 (d, 1 H, J = 3.0 Hz), 8.56 (d, 1 H, J = 4.8 Hz), 8.41 (m, 3 H), 8.23 (d, 1 H, J = 8.4 Hz), 7.95 (t, 1 H, J = 8.7 Hz), 4.48 (m, 1 H), 4.40 (t, 2 H, J = 6.0 Hz), 3.46 (t, 2 H, J = 5.1 Hz), 2.90 (d, 6 H, J = 4.5 Hz), 1.61 (d, 3 H, J = 6.6 Hz); ^{13}C-NMR (DMSO, 150 MHz): δ 170.3, 164.5, 163.9, 139.8, 131.9, 131.6, 130.3, 129.0, 127.2, 125.2, 123.0, 121.1, 119.3, 54.6, 49.5, 42.6, 35.4, 17.8; HRMS (ESI) m/z calcd for $C_{19}H_{23}N_4O_3$ ($[M + H]^+$) 355.1765; found 355.1759.

3. Spectroscopic materials and methods

Buffer reagents were purchased from Aldrich and Acros and were used without purification. Water used for the fluorescence studies was doubly distilled and further purified with a Mill-Q filtration system. Absorption spectra were recorded using Shimadzu UV-1700 UV-visible spectrometer. Fluorescence spectra were recorded using Varioskan microplate reader (Thermo Electron Corporation). Solutions of compounds **6c**, **6d** and **6e** were prepared in 0.1 M Tris-HCl buffer at pH 7.5. Solutions of compounds **2a** and **2b** were prepared in 0.1 M Tris-HCl (contains 1% DMSO) buffer at pH 7.5

4. V_{max} and K_m measurement

Kinetic constants (V_{max} and K_m) were determined by following the methods described in the literature.[26] For **6c**, **6d** and **6e**, an enzyme concentration of 0.2 IU mL^{-1} and [S] final between 0.025 and 0.80 mM were used. For substrate L-Leu-*p*-nitroanilide, an enzyme concentration of 0.05 IU mL^{-1} and [S] final between 0.025 and 1.6 mM were used. The assays were performed in quadruplicate. K_m and V_{max} were calculated by the Lineweaver–Burk plot by using SigmaPlot 12 (Fig. S2‡).

5. Cell culture and fluorescent image assay

Human non-T, non-B acute lymphoblastic leukemia cells (REH) were grown in RPMI-1640 medium supplemented with 10% (v/v) fetal bovine serum, 1.5 g L^{-1} $NaHCO_3$, 2.5 g L^{-1} glucose, 0.11 g L^{-1} sodium pyruvate in an atmosphere of 5% CO_2, 95% air at 37 °C. Human ovarian clear cell carcinoma cells (ES-2) were grown in RPMI-1640 medium supplemented with 10% (v/v) fetal bovine serum in an atmosphere of 5% CO_2, 95% air at 37 °C. For the cellular level APN activity assay, ES-2 and REH cells were respectively centrifuged for 400 s at 800 rpm, and then suspended with RPMI-1640 medium. The mixture of 200 μL of the above RPMI-1640 medium suspension with 6 × 10^5 or 3 × 10^5 cells and 10 μL **6e** (1.4 mM) were incubated at 37 °C for 1 h. The fluorescence intensities were recorded using a Varioskan microplate reader. For the fluorescent image assay, after the medium was removed, the cells were carefully washed with RPMI-1640 medium, and then incubated at r.t. in the presence of probe **6e** (5 μM) or the mixture of probe **6e** (5 μM) and Bestatin (4.9 mM) in RPMI-1640 medium for 5 min. Fluorescence imaging was performed using an OLYMPUS CK30-F200 fluorescence microscope. Ratiometric pictures were achieved with ImageJ software.[27]

Acknowledgements

The present work was supported by the Program for New Century Excellent Talents in University (No. NCET-11-0306), the Shandong Natural Science Foundation (No. JQ201019), the Independent Innovation Foundation of Shandong University, IIFSDU (No. 2010JQ005) and the Graduate Independent Innovation Foundation of Shandong University, GIIFSDU (No. yzc12096).

Notes and references

1 L. Chen, Y. Teng and W. Xu, *Curr. Med. Chem.*, 2011, **18**, 964–976.
2 B. Bauvois and D. Dauzonne, *Med. Res. Rev.*, 2006, **26**, 88–130.
3 M. Piedfer, D. Dauzonne, R. Tang, J. N'Guyen, C. Billard and B. Bauvois, *FASEB J.*, 2011, **25**, 2831–2842.
4 J. Zhang, X. Li, H. W. Zhu, Q. Wang, J. H. Feng, J. J. Mou, Y. G. Li, H. Fang and W. F. Xu, *Drug Discovery Ther.*, 2010, **4**, 5–12.
5 I. Y, T. W, Z. L, D. G, X. W and K. N, *Biosci. Trends*, 2010, **4**, 56–60.
6 M. Wickström, K. Viktorsson, L. Lundholm, R. Aesoy, H. Nygren, L. Sooman, M. Fryknäs, L. K. Vogel, R. Lewensohn, R. Larsson and J. Gullbo, *Biochem. Pharmacol.*, 2010, **79**, 1281–1290.
7 F. Curnis, A. Sacchi, L. Borgna, F. Magni, A. Gasparri and A. Corti, *Nat. Biotechnol.*, 2000, **18**, 1185–1190.
8 R. E. Wang, Y. Niu, H. Wu, Y. Hu and J. Cai, *Anti-Cancer Agents Med. Chem.*, 2012, **12**, 76–86.
9 N. Haraguchi, H. Ishii, K. Mimori, F. Tanaka, M. Ohkuma, H. M. Kim, H. Akita, D. Takiuchi, H. Hatano, H. Nagano, G. F. Barnard, Y. Doki and M. Mori, *J. Clin. Invest.*, 2010, **120**, 3326–3339.
10 A. Corti, F. Curnis, W. Arap and R. Pasqualini, *Blood*, 2008, **112**, 2628–2635.
11 A. von Wallbrunn, J. Waldeck, C. Holtke, M. Zuehlsdorf, R. Mesters, W. Heindel, M. Schafers and C. Bremer, *J. Biomed. Opt.*, 2008, **13**, 011007/1–011007/9.
12 Z. Zhang, H. Harada, K. Tanabe, H. Hatta, M. Hiraoka and S.-i. Nishimoto, *Peptides*, 2005, **26**, 2182–2187.
13 A. Buehler, M. A. M. J. van Zandvoort, B. J. Stelt, T. M. Hackeng, B. H. G. J. Schrans-Stassen, A. Bennaghmouch, L. Hofstra, J. P. M. Cleutjens, A. Duijvestijn, M. B. Smeets, D. P. V. de Kleijn, M. J. Post and E. D. de Muinck, *Arterioscler., Thromb., Vasc. Biol.*, 2006, **26**, 2681–2687.
14 F. Curnis, G. Arrigoni, A. Sacchi, L. Fischetti, W. Arap, R. Pasqualini and A. Corti, *Cancer Res.*, 2002, **62**, 867–874.
15 A. H. Negussie, J. L. Miller, G. Reddy, S. K. Drake, B. J. Wood and M. R. Dreher, *J. Controlled Release*, 2010, **143**, 265–273.
16 F. Noble, N. Luciani, S. Da Nascimento, R. Laï-Kuen, L. Bischoff, H. Chen, M.-C. Fournié-Zaluski and B. P. Roques, *FEBS Lett.*, 2000, **467**, 81–86.
17 F. Noble, G. Banisadr, F. Jardinaud, T. Popovici, R. Lai-Kuen, H. Chen, L. Bischoff, S. M. Parsadaniantz, M. C. Fournie-Zaluski and B. P. Roques, *Neuroscience*, 2001, **105**, 479–488.
18 R. A. Smith and T. D. Giorgio, *Cytometry, Part A*, 2009, **75**, 465–474.
19 H. Kobayashi, M. Ogawa, R. Alford, P. L. Choyke and Y. Urano, *Chem. Rev.*, 2009, **110**, 2620–2640.
20 L. Yuan, W. Lin, Y. Xie, B. Chen and J. Song, *Chem. Commun.*, 2011, **47**, 9372–9374.
21 J. Jiang, W. Liu, J. Cheng, L. Yang, H. Jiang, D. Bai and W. Liu, *Chem. Commun.*, 2012, **48**, 8371–8373.
22 L. Chen, W. Sun, W. Li, J. Li, L. Du, W. Xu, H. Fang and M. Li, *Anal. Methods*, 2012, **4**, 2661–2663.
23 W. Sun, W. Li, J. Li, J. Zhang, L. Du and M. Li, *Tetrahedron*, 2012, **68**, 5363–5367.
24 B. Zhu, X. Zhang, Y. Li, P. Wang, H. Zhang and X. Zhuang, *Chem. Commun.*, 2010, **46**, 5710–5712.
25 M. Drag, M. Bogyo, J. A. Ellman and G. S. Salvesen, *J. Biol. Chem.*, 2010, **285**, 3310–3318.
26 H. Huang, H. Tanaka, B. D. Hammock and C. Morisseau, *Anal. Biochem.*, 2009, **391**, 11–16.
27 J. Kardash, E. Fau-Bandemer, E. Bandemer, J. Fau-Raz and R. E, *Nat. Protoc.*, 2011, **6**, 1835–1846.

